



# Gold Nanoparticles: Enhancing the Sensitivity of Clinical Diagnostic Tests

## Free Article Collection eBook

The current COVID-19 pandemic has brought much attention to the medical utility of rapid diagnostic test (RDTs). Although these assays are easy to use and provide fast diagnostic results at the point-of-care, one of the main limitations in their development has been the prevalence of false-positive and false-negative results. To improve their sensitivity, gold nanoparticle probes have been incorporated into the design of RDTs. Gold nanoparticles are highly regarded for their optoelectronic properties, biocompatibility, stability, and their ability to be synthesized into various shapes.

Taken together, these features can be utilized in various combinations to optimize the sensitivity and accuracy of clinical diagnostics. Our article collection "Gold Nanoparticles: Enhancing the Sensitivity of Clinical Diagnostic Tests" highlights several applications where gold nanoparticles were used to improve clinical biomarker or disease detection.

**Through this research article collection, we hope to educate scientists on how gold nanoparticles can be used to enhance the sensitivity of clinical diagnostic tests.**

[Download here](#)

# Integration of Highly Luminescent Lead Halide Perovskite Nanocrystals on Transparent Lead Halide Nanowire Waveguides through Morphological Transformation and Spontaneous Growth in Water

Tao Chen, Chong Wang,\* Xinxin Xing, Zhaojun Qin, Fan Qin, Yanan Wang, Md Kamrul Alam, Viktor G. Hadjiev, Guang Yang, Shuming Ye, Jie Yang, Rongfei Wang, Shuai Yue, Di Zhang, Zhongxia Shang, Francisco C. Robles-Hernandez, Hector A. Calderon, Haiyan Wang, Zhiming Wang, and Jiming Bao\*

The integration of highly luminescent  $\text{CsPbBr}_3$  quantum dots on nanowire waveguides has enormous potential applications in nanophotonics, optical sensing, and quantum communications. On the other hand,  $\text{CsPb}_2\text{Br}_5$  nanowires have also attracted a lot of attention due to their unique water stability and controversial luminescent property. Here, the growth of  $\text{CsPbBr}_3$  nanocrystals on  $\text{CsPb}_2\text{Br}_5$  nanowires is reported first by simply immersing  $\text{CsPbBr}_3$  powder into pure water,  $\text{CsPb}_{3-\gamma}\text{X}_\gamma$  ( $\text{X} = \text{Cl, I}$ ) nanocrystals on  $\text{CsPb}_{2\gamma}\text{Br}_{5-\gamma}\text{X}_\gamma$  nanowires are then synthesized for tunable light sources. Systematic structure and morphology studies, including *in situ* monitoring, reveal that  $\text{CsPbBr}_3$  powder is first converted to  $\text{CsPb}_2\text{Br}_5$  microplatelets in water, followed by morphological transformation from  $\text{CsPb}_2\text{Br}_5$  microplatelets to nanowires, which is a kinetic dissolution–recrystallization process controlled by electrolytic dissociation and supersaturation of  $\text{CsPb}_2\text{Br}_5$ .  $\text{CsPbBr}_3$  nanocrystals are spontaneously formed on  $\text{CsPb}_2\text{Br}_5$  nanowires when nanowires are collected from the aqueous solution. Raman spectroscopy, combined photoluminescence, and SEM imaging confirm that the bright emission originates from  $\text{CsPb}_{3-\gamma}\text{X}_\gamma$  nanocrystals while  $\text{CsPb}_{2\gamma}\text{Br}_{5-\gamma}\text{X}_\gamma$  nanowires are transparent waveguides. The intimate integration of nanoscale light sources with a nanowire waveguide is demonstrated through the observation of the wave guiding of light from nanocrystals and Fabry–Perot interference modes of the nanowire cavity.

## 1. Introduction

The integration of highly efficient fluorescent semiconductor nanocrystals or quantum dots with sub-micrometer waveguides is essential to the construction of photonic circuits for a wide range of applications in quantum information, optical communication and sensing.<sup>[1–6]</sup> Even although a few integration techniques have been developed over the years, for example, by physically placing nanocrystals to a waveguide,<sup>[4,7,8]</sup> chemically adsorption of nanocrystals on a waveguide<sup>[9,10]</sup> or using e-beam lithography<sup>[11,12]</sup> to define and control relative position of nanocrystals and waveguides, the integration still remains challenging, since it involves precise manipulation of nanoscale objects. All-inorganic lead halide perovskite  $\text{CsPbBr}_3$  quantum dots, because of their nearly 100% quantum efficiency,<sup>[13,14]</sup> have emerged as an ideal candidate for non-classical light source.<sup>[10,15–19]</sup> In particular, by integrating quantum dots with a waveguide, a single photon quantum source has been demonstrated.<sup>[20,21]</sup>

T. Chen, C. Wang, S. M. Ye, J. Yang, R. F. Wang  
National Center for International Research on Photoelectric and  
Energy Materials  
School of Materials and Energy  
Yunnan University  
Kunming 650091, P. R. China  
E-mail: cwang@ynu.edu.cn

X. Xing, Z. J. Qin, F. Qin, Y. Wang, M. K. Alam, G. Yang, S. Yue,  
F. C. Robles-Hernandez, J. M. Bao  
Department of Electrical and Computer Engineering  
University of Houston  
Houston, TX 77204, USA  
E-mail: jbao@central.uh.edu

 The ORCID identification number(s) for the author(s) of this article  
can be found under <https://doi.org/10.1002/smll.202105009>.

DOI: 10.1002/smll.202105009

X. Xing, Z. J. Qin, S. Yue, Z. M. Wang  
Institute of Fundamental and Frontier Sciences  
University of Electronic Science and Technology of China  
Chengdu, Sichuan 610054, P. R. China

V. G. Hadjiev  
Department of Mechanical Engineering  
University of Houston  
Houston, TX 77204, USA

V. G. Hadjiev, J. M. Bao  
Texas Center for Superconductivity  
University of Houston  
Houston, TX 77204, USA

D. Zhang, Z. X. Shang, H. Y. Wang  
School of Materials Engineering  
Purdue University  
West Lafayette, IN 47907, USA

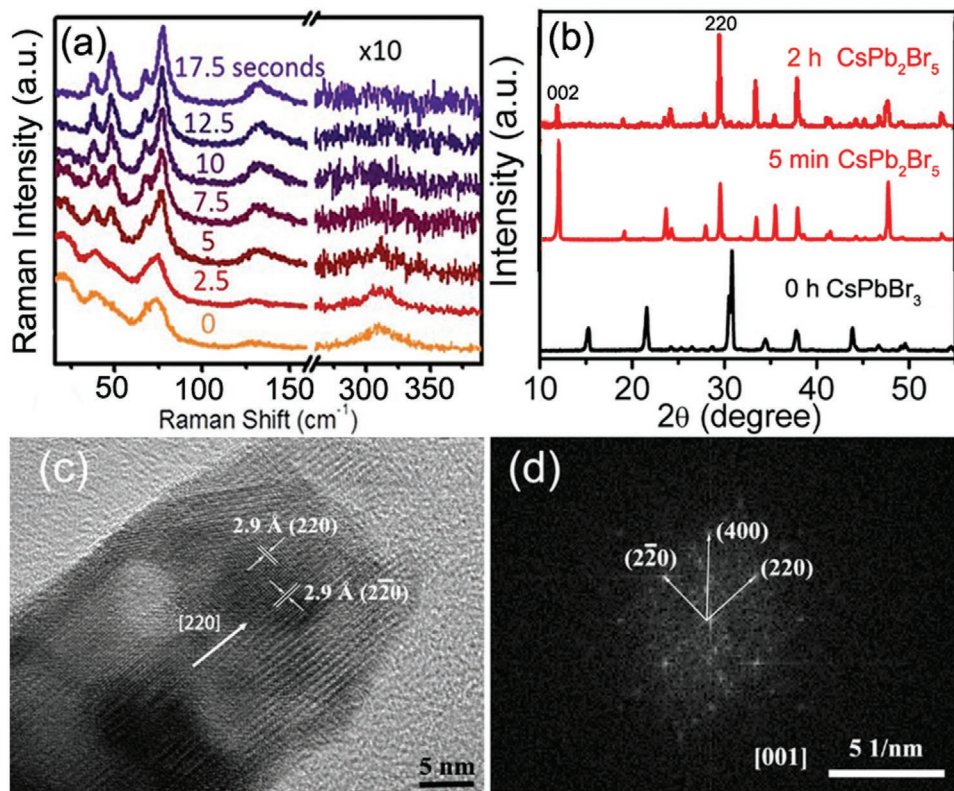


**Figure 1.** Raman, XRD and TEM characterizations of  $\text{CsPb}_2\text{Br}_5$  nanowires. a) Evolution of Raman spectrum at room temperature when a droplet of water was added to  $\text{CsPbBr}_3$  powder. b) XRD spectra of dry precipitates produced after immersing  $\text{CsPbBr}_3$  powder in water with different immersion times. c) Representative HR-TEM image of a  $\text{CsPb}_2\text{Br}_5$  nanowire and d) the corresponding fast Fourier transform (FFT) image.

Lead halide  $\text{CsPb}_2\text{Br}_5$  perovskite has also attracted a lot of attention due to several reasons. First, unlike most lead halide perovskites, it is a water-stable wide band gap semiconductor.<sup>[22–27]</sup> Highly environment-stable lasers and light emitting diodes (LEDs) have been demonstrated by embedding perovskite nanocrystals such as  $\text{CsPbBr}_3$  in transparent  $\text{CsPb}_2\text{Br}_5$  matrix.<sup>[28–34]</sup> Second, as an intrinsic layered material,  $\text{CsPb}_2\text{Br}_5$  can be synthesized in the form of 2D platelets or 1D nanowires, thus enabling more applications in nanophotonics. Finally, the origin of its bright green emission has been the center of heated debates and still requires further investigation.<sup>[22,24,35–41]</sup> In our previous work, we showed that  $\text{CsPbBr}_3$  and  $\text{CsPbBr}_{3-\gamma}\text{X}_\gamma$  ( $\text{X} = \text{Cl, I}$ ) nanocrystals rather than Br vacancies are responsible for the tunable visible light emission in  $\text{CsPb}_2\text{Br}_5$  platelets.<sup>[27]</sup> This discovery can be applied to emissive  $\text{CsPb}_2\text{Br}_5$  and  $\text{CsPb}_2\text{Br}_{5-\gamma}\text{X}_\gamma$  nanowires in principle, but a direct observation of  $\text{CsPbBr}_3$  and  $\text{CsPbBr}_{3-\gamma}\text{X}_\gamma$  nanocrystals has not been confirmed.<sup>[42,43]</sup> As such, the origin of the visible emission remains yet to be determined.

F. C. Robles-Hernandez  
Mechanical Engineering Technology  
University of Houston  
Houston, TX 77204, USA

H. A. Calderon  
Institute Politecnico Nacional  
ESFM-IPN  
UPALM  
Departamento de Física  
Mexico CDMX 07338, Mexico

In this work, we discovered a catalyst- and ligand-free method to synthesize  $\text{CsPb}_2\text{Br}_5$  nanowires with or without decorated  $\text{CsPbBr}_3$  nanocrystals. The nanowires were grown from the water solution of  $\text{CsPb}_2\text{Br}_5$  platelets through a morphological transformation. Raman spectroscopy, same-spot photoluminescence imaging and scanning electron microscopy (SEM) confirmed that pure  $\text{CsPb}_2\text{Br}_5$  nanowires have no green photoluminescence, and the decorated  $\text{CsPbBr}_3$  nanocrystals are responsible for the green emissive  $\text{CsPb}_2\text{Br}_5$  nanowires. Highly luminescent  $\text{CsPb}_2\text{Br}_{5-\gamma}\text{X}_\gamma$  nanowires were also synthesized and the same conclusion as above was obtained. The integrated  $\text{CsPbBr}_3/\text{CsPb}_2\text{Br}_5$  NC/NW exhibits a dual function as a waveguide-coupled light source and an optical Fabry–Perot cavity.

## 2. Results and Discussion

$\text{CsPb}_2\text{Br}_5$  platelets were first synthesized using the same method as before by simply dropping  $\text{CsPbBr}_3$  micro-cubes (or powders) in a large quantity of pure water (>20 times in mass) in a flask or bottle at room temperature.<sup>[27]</sup> Similar water-triggered phase transformation has also been reported,<sup>[44–48]</sup> the transformation is due to a high solubility of  $\text{CsPbBr}_3$  and a much lower solubility of  $\text{CsPb}_2\text{Br}_5$  in water,  $\text{CsPb}_2\text{Br}_5$  can be formed in seconds and become a white precipitate from the initial yellow  $\text{CsPbBr}_3$  powders. This rapid structural conversion in water can be verified by in situ Raman spectroscopy. Figure 1a shows the evolution of Raman spectrum when a

small water droplet was added to  $\text{CsPbBr}_3$  powders. The dissolution of  $\text{CsPbBr}_3$  can be seen from the disappearance of its characteristic Raman peak at  $310 \text{ cm}^{-1}$ , and the emergence of  $\text{CsPb}_2\text{Br}_5$  is manifested by the appearance of sharp Raman features below 100 and  $133 \text{ cm}^{-1}$ .

To obtain  $\text{CsPb}_2\text{Br}_5$  nanowires, we replaced the solution with fresh water while keeping the platelet precipitates at the bottom, then heated up the water with stirring on a hot plate. When the temperature reached  $60^\circ\text{C}$  (in about 15 min), we stopped heating and stirring, let the solution cool down naturally. The formation of  $\text{CsPb}_2\text{Br}_5$  nanowires can be revealed by a subtle change in X-ray diffraction (XRD) in Figure 1b: the relative intensity of (220) to (002) increases dramatically when the immersion time increases from 5 min to 2 h, here the immersion time was counted from the exchange of water and beginning of the heating. The strong (002) peak in the 5 min immersion sample is due to the intrinsic 2D layered structure of  $\text{CsPb}_2\text{Br}_5$  platelets. The strong (220) peak in 2 h sample indicates another preferred growth direction of  $\text{CsPb}_2\text{Br}_5$  nanowires, which is confirmed by the high-resolution transmission electron microscopy (HR-TEM) image and corresponding fast Fourier transform (FFT) pattern shown in Figures 1c,d.

To obtain a better understanding of  $\text{CsPb}_2\text{Br}_5$  nanowire growth from  $\text{CsPb}_2\text{Br}_5$  2D platelets, we monitored morphology evolution of  $\text{CsPb}_2\text{Br}_5$  precipitates with increasing immersion time. Figure 2a-d shows representative optical images of  $\text{CsPb}_2\text{Br}_5$  nanowires from exchange of water to 4 h of imme-

rsion time. We observed that, first, unlike platelets, the growth of nanowires takes time. More nanowires will be formed as immersion time increases and a complete conversion to nanowires can also be achieved after 4 h, which can be conveniently recognized by a milky white color of suspended  $\text{CsPb}_2\text{Br}_5$  nanowires in Figure 2e. Second, these nanowires do not seem to grow from platelets since they are not attached to platelets. The latter observation is also confirmed by the in situ observations of nanowire growth in solution. Figure 2f,g shows optical images when a droplet of clean  $\text{CsPb}_2\text{Br}_5$  water solution is left on a glass slide in air. As the droplet dries up, two nanowires appear and grow. A faster growth here is due to increased ion concentration as a result of quick evaporation of water in air. Figure 2h,i shows SEM images of nanowires. It can be seen that nanowires are not tapered and can have diameter much less than 1  $\mu\text{m}$ , but as optical pictures have also revealed, their lengths are not uniform.

Solution synthesis is a very common method to grow nanostructures. However, spontaneous morphological transformation in solution is rarely reported.<sup>[33,49–51]</sup> If it happens, typically one type of nanostructures will grow from the other structures. For example,  $\text{CeO}_2$  nanorods can grow on  $\text{CeO}_2$  nanooctahedrons through the dissolution of the nano-octahedrons and recrystallization of the nanorods.<sup>[52]</sup>  $\text{CsPbBr}_3$  nanowires are formed through oriented self-assembly of  $\text{CsPbBr}_3$  nanocubes in solution.<sup>[53]</sup> Moreover, most anisotropic growth during the phase conversion takes place via solution method by adding complex ligands in the material synthetic process.<sup>[54,55]</sup> In

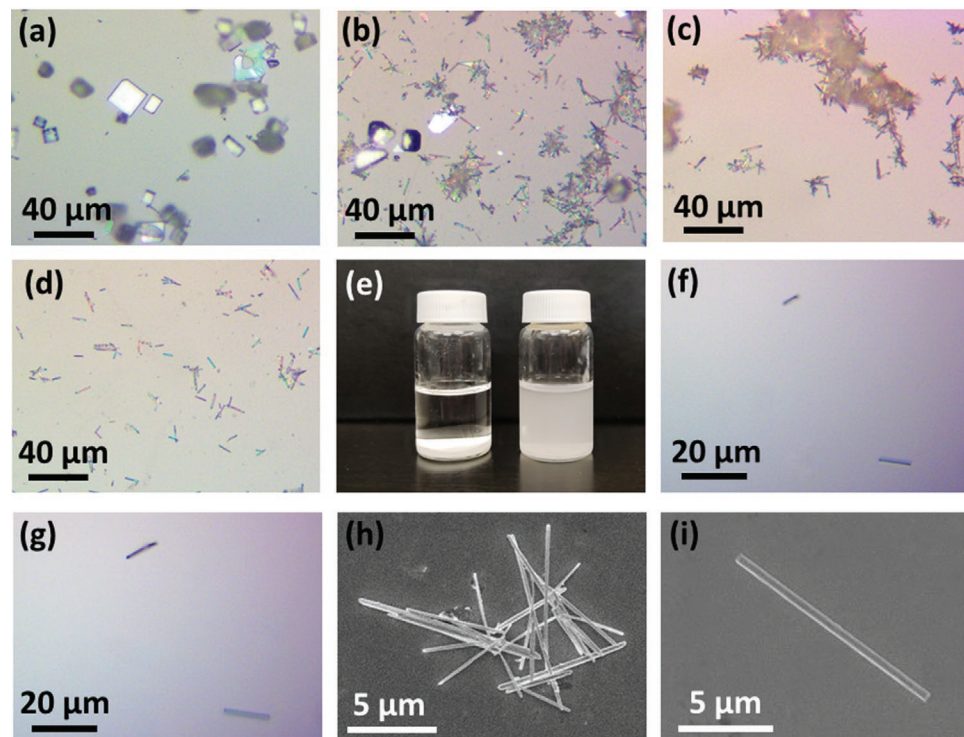


**Figure 2.** Optical and SEM images of  $\text{CsPb}_2\text{Br}_5$  nanowires. a–d) Optical images of  $\text{CsPb}_2\text{Br}_5$  after exchange of water for a) 0 h, b) 1 h, c) 3 h, and d) 4 h. e) Pictures of water right after dropping off  $\text{CsPbBr}_3$  (left) and after the conversion of  $\text{CsPb}_2\text{Br}_5$  platelets to nanowires in 4 h (right). f,g) In situ observation of the growth of  $\text{CsPb}_2\text{Br}_5$  nanowires from  $\text{CsPb}_2\text{Br}_5$  saturated water. Picture in g) was taken about 10 min after the picture in f). h,i) SEM images of  $\text{CsPb}_2\text{Br}_5$  nanowires from (e).

our case, nanowires and platelets are completely separated, and nanowires grow out of solution from  $\text{Cs}^+$ ,  $\text{Pb}^{2+}$ ,  $\text{Br}^-$  ions in water, which can be described as a dissolution-recrystallization during the transformation from  $\text{CsPb}_2\text{Br}_5$  plates to nanowires.<sup>[33,49–51,56]</sup> According to recent work by Lai et al.,<sup>[56]</sup> the crystallization morphology is controlled by supersaturation for a material that has a low electrolytic dissociation, such as  $\text{CsPb}_2\text{Br}_5$  due to its low solubility in water. As such, a rapid recrystallization by dropping  $\text{CsPbBr}_3$  powder in water will result in 2D  $\text{CsPb}_2\text{Br}_5$  platelets, while 1D  $\text{CsPb}_2\text{Br}_5$  nanowires will be formed due to slow cooling of  $\text{CsPb}_2\text{Br}_5$  saturated aqueous solution.

$\text{CsPb}_2\text{Br}_5$  nanowires were reported to exhibit strong green photoluminescence (PL).<sup>[42,43]</sup> This is confirmed in Figure 3a,b if we simply take the wires out of the water and let them dry. However, our previous work has shown that if the  $\text{CsPb}_2\text{Br}_5$  platelets are carefully washed by water and ethanol,  $\text{CsPbBr}_3$  nanocrystals cannot be formed on the surface of  $\text{CsPb}_2\text{Br}_5$  platelets; subsequently, their green photoluminescence can be eliminated. To investigate the effect of postsynthesis drying on the optical property, we performed similar cleaning and drying steps. The results in Figure 3c,d confirmed our previous observations: the cleaned nanowires showed no PL emission. Following the same

procedure as before, we compared Raman spectra of emissive and nonemissive nanowires, and we performed photoluminescence imaging and SEM imaging on the same nanowires to further verify  $\text{CsPbBr}_3$  nanocrystals as the source of the green emission. SEM and PL images in Figure 3e–k confirm that overgrown nanocrystal bumps on nanowires are responsible for the green emission, and Raman spectra in Figure 3l confirms these bumps as  $\text{CsPbBr}_3$  nanocrystals from their characteristic Raman line at  $310 \text{ cm}^{-1}$ .

Having determined that  $\text{CsPbBr}_3$  nanocrystals are responsible for the strong green emission in  $\text{CsPb}_2\text{Br}_5$  nanowires, we believe that the previously observed emission in  $\text{CsPb}_2\text{Br}_{5-\gamma}\text{X}_\gamma$  nanowires was also due to  $\text{CsPb}_{3-\gamma}\text{X}_\gamma$ . We can use two synthesis methods to prove this hypothesis. The first is to use the emissive  $\text{CsPb}_2\text{Br}_5$  nanowires and ion exchange to partially replace  $\text{Br}^-$  with  $\text{Cl}^-$  or  $\text{I}^-$  in  $\text{CsPbBr}_3/\text{CsPb}_2\text{Br}_5$ , as we did for  $\text{CsPb}_2\text{Br}_5$  platelets and ion exchange only took place on the surface of the  $\text{CsPb}_2\text{Br}_5$  platelets.<sup>[27]</sup> The second approach is to synthesize  $\text{CsPb}_{3-\gamma}\text{X}_\gamma$  first and then use water to convert  $\text{CsPb}_{3-\gamma}\text{X}_\gamma$  to  $\text{CsPb}_{2\gamma}\text{Br}_{5-\gamma}\text{X}_\gamma$ . Here we use the latter method, the detailed procedures are described in Experimental Section. The successful incorporation of Cl or I into  $\text{CsPb}_2\text{Br}_5$  crystal lattice can be seen from

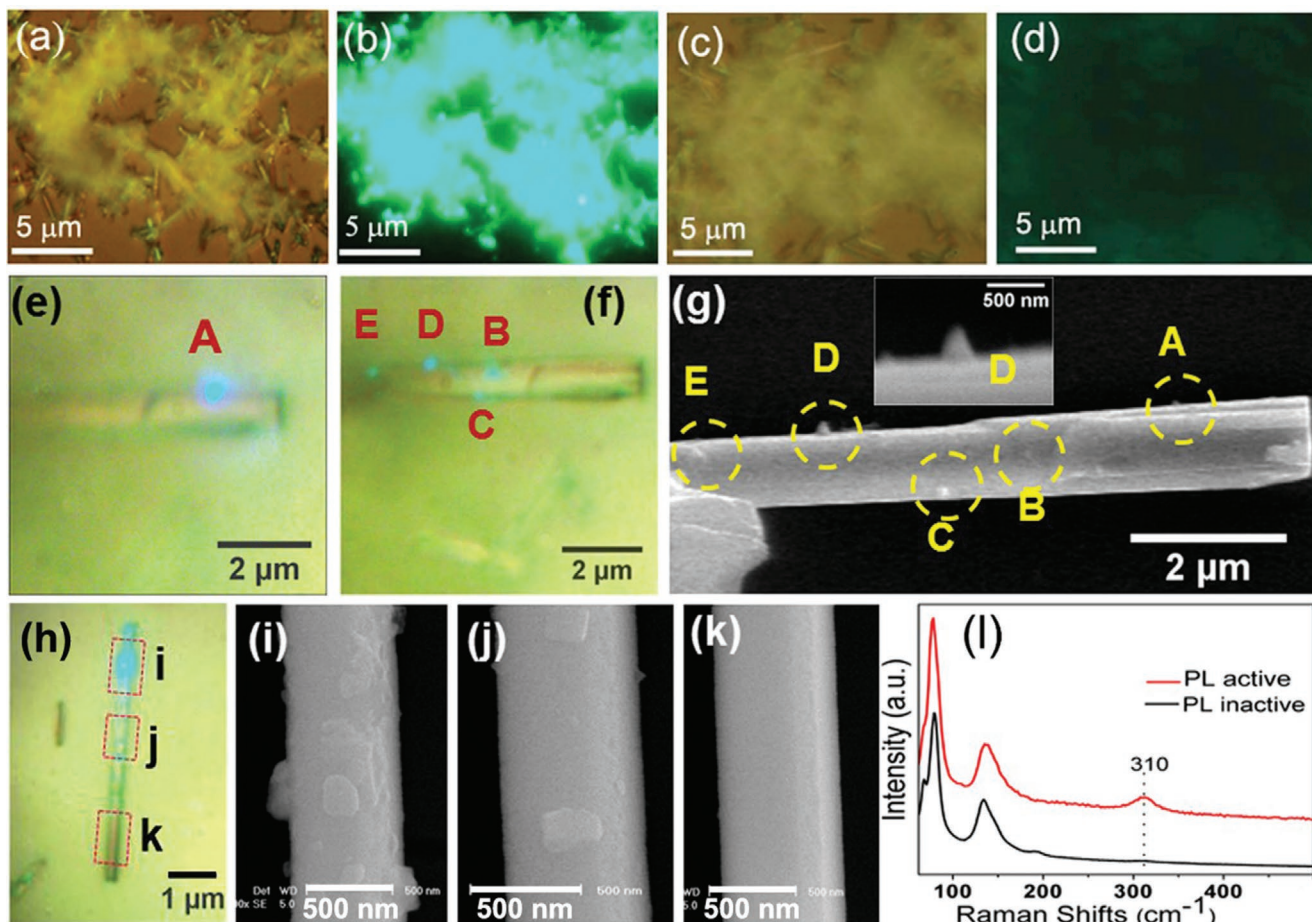


**Figure 3.** Optical, photoluminescence, and SEM images, as well as Raman spectra of  $\text{CsPb}_2\text{Br}_5$  nanowires. Optical images of  $\text{CsPb}_2\text{Br}_5$  nanowires a) without and c) with cleaning. b,d) Corresponding photoluminescence images. e–g,h–k) Photoluminescence and SEM images of two individual nanowires. l) Raman spectra of PL-active site and PL-inactive site of the same nanowire.

slightly shifted XRD peaks in Figure 4a.<sup>[42]</sup> The diffraction angles of  $\text{CsPb}_2\text{Br}_{5-\gamma}\text{I}_\gamma$  ( $\text{CsPb}_2\text{Br}_{5-\gamma}\text{Cl}_\gamma$ ) are reduced (increased) due to a larger (smaller) size of I (Cl) ions and subsequently a larger (smaller) lattice constant. This is different from the ion exchange using emissive  $\text{CsPb}_2\text{Br}_5$  platelets, where no obvious change of lattice constant was observed.<sup>[27]</sup> We believe that ion exchange happened mainly to the surface  $\text{CsPbBr}_3$  nanocrystals instead  $\text{CsPb}_2\text{Br}_5$  platelets.<sup>[27]</sup> Following the same PL imaging and Raman spectroscopy technique, we can deter-

mine the origin of new luminescent centers. Specifically, PL images from individual nanowires in Figure 4b,c show that the emission does not come from the whole body of nanowires, but, instead from discrete bumps on the nanowires, which indicates that  $\text{CsPb}_2\text{Br}_{5-\gamma}\text{X}_\gamma$  nanowires have no photoluminescence as  $\text{CsPb}_2\text{Br}_5$  nanowires. Similar to  $\text{CsPb}_2\text{Br}_5$  nanowires, PL of  $\text{CsPb}_2\text{Br}_{5-\gamma}\text{X}_\gamma$  nanowires originated from the  $\text{CsPbBr}_{3-\gamma}\text{X}_\gamma$  nanocrystals, which exhibit a blue or red spectral shift compared to that of  $\text{CsPbBr}_3$ , as shown in Figure 4d.<sup>[27]</sup>

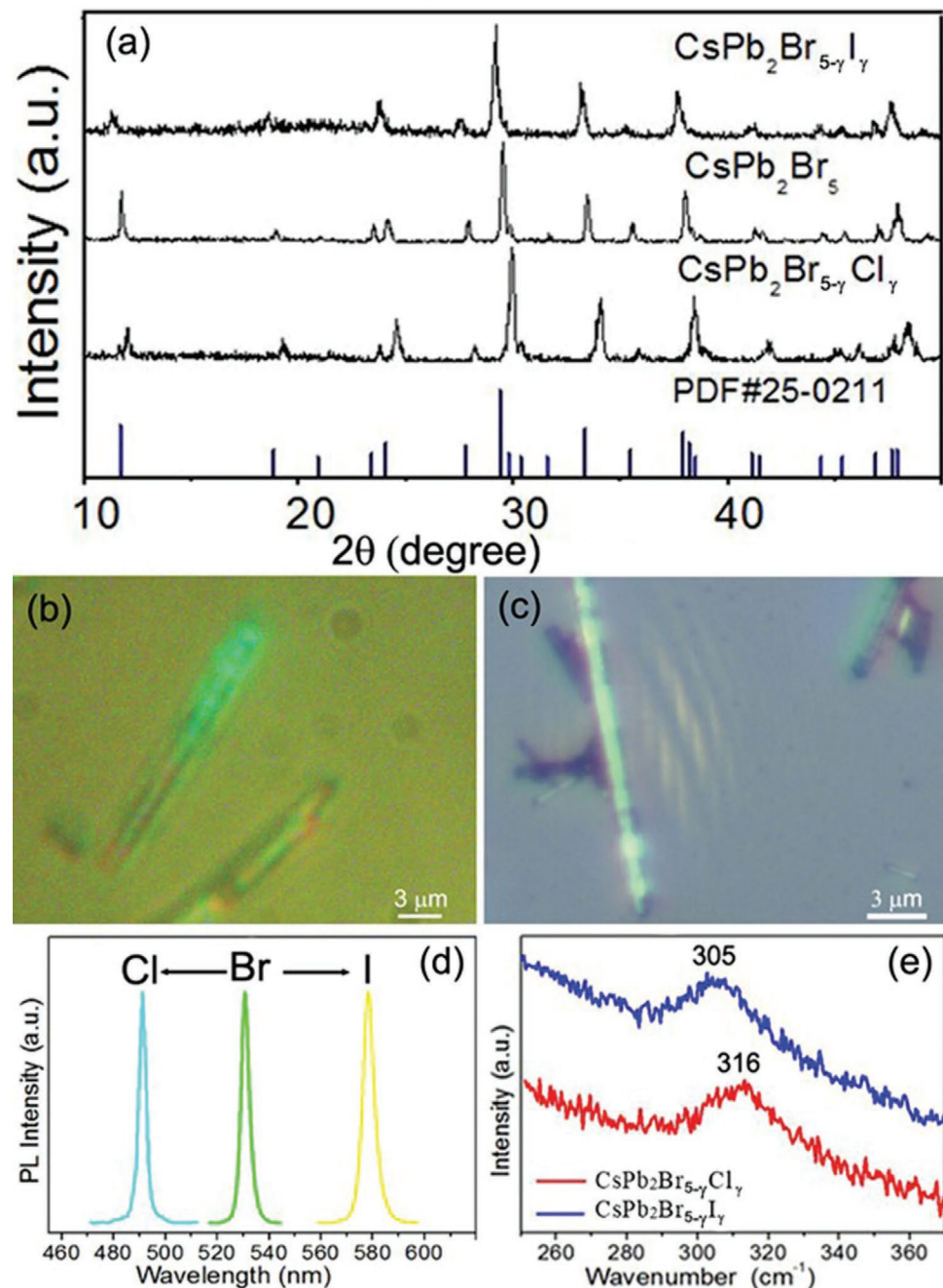


**Figure 4.** XRD, photoluminescence and Raman spectra of  $\text{CsPbBr}_{3-\gamma}\text{X}_\gamma$  nanowires. a) XRD of  $\text{CsPb}_2\text{Br}_5$ ,  $\text{CsPb}_2\text{Br}_{5-\gamma}\text{Cl}_\gamma$  and  $\text{CsPb}_2\text{Br}_{5-\gamma}\text{I}_\gamma$  nanowires. b, c) Photoluminescence images of b)  $\text{CsPb}_2\text{Br}_{5-\gamma}\text{Cl}_\gamma$  and c)  $\text{CsPb}_2\text{Br}_{5-\gamma}\text{I}_\gamma$ . d) Representative PL spectra of emissive  $\text{CsPb}_2\text{Br}_{5-\gamma}\text{X}_\gamma$ . e) Raman spectra of PL-active  $\text{CsPb}_2\text{Br}_{5-\gamma}\text{Cl}_\gamma$  and  $\text{CsPb}_2\text{Br}_{5-\gamma}\text{I}_\gamma$  nanowires.

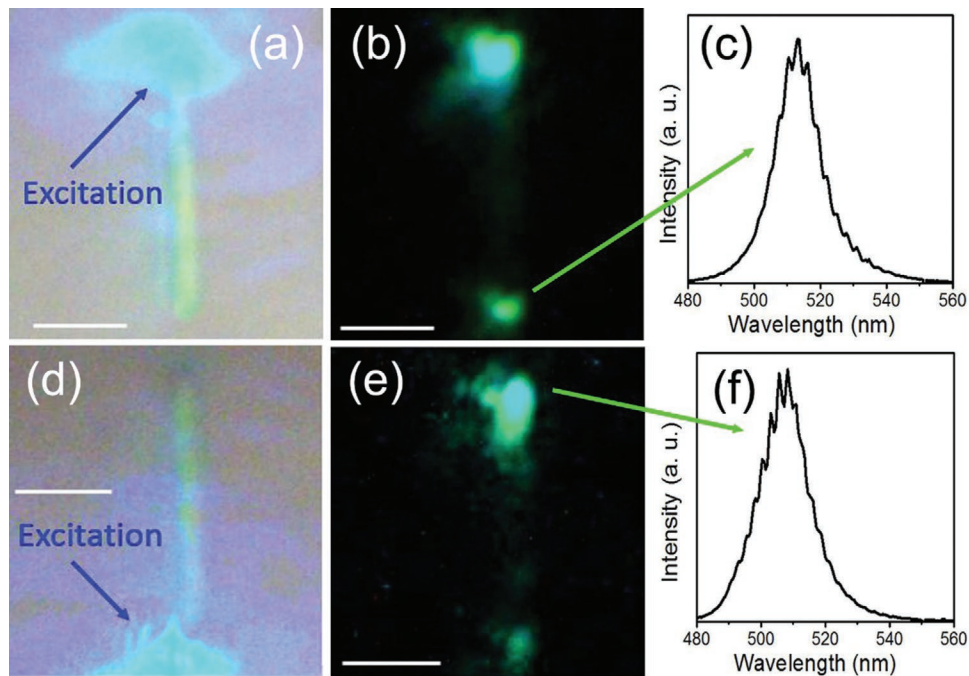


**Figure 5.** Optical coupling of  $\text{CsPbBr}_3$  nanocrystals to  $\text{CsPb}_2\text{Br}_5$  nanowire waveguide. a,d) Optical image of a  $\text{CsPb}_2\text{Br}_5$  nanowire under white light illumination and 473-nm laser excitation from a) the top end and d) the bottom end. b,e) Corresponding photoluminescence images of (a) and (d) when the white light is turned off and laser is filtered out. c,f) Spectra of transmitted photoluminescence. Scale bar: 5  $\mu\text{m}$ .

This conclusion is further supported by observations of Raman signature of  $\text{CsPbBr}_{3-\gamma}\text{X}_\gamma$  nanocrystals shown in Figure 4e.<sup>[27]</sup>

The integration of a nanoscale light emitter with a nanowire waveguide is the basic requirement for a nanophotonic circuit. Here we demonstrate two basic functions of  $\text{CsPbBr}_3/\text{CsPb}_2\text{Br}_5$  nanocrystal/nanowire (NC/NW) as a waveguide and a light source. This can be done after we transfer a single  $\text{CsPbBr}_3/\text{CsPb}_2\text{Br}_5$  NC/NW onto a  $\text{CaF}_2$  substrate. Figure 5a,b shows optical image of the NC/NW, where its top  $\text{CsPbBr}_3$  end is excited by a laser beam. The coupling of excited green luminescence to the nanowire waveguide and its propagation to the bottom clean end can be seen from a visible but relatively weaker green spot. When the nanowire is excited from the bottom clean end, Figure 5d,e show a similar luminescence image: a stronger green emission on the top end and a relatively weak spot at the bottom end. This is because the top end has  $\text{CsPbBr}_3$  nanocrystals. However, the way the  $\text{CsPbBr}_3$  nanocrystals are excited is very different; in this case, it is the laser that couples to the nanowire, propagates to the top end, and excites the nanocrystals. Despite this different excitation method, Figure 5c,f and Figure S1 in the Supporting Information show that the green emission spectra exhibit well-known Fabry–Perot interference fringes, indicating a high nanowire optical cavity.

### 3. Conclusions

In summary, we discovered a platelet-to-nanowire morphological transformation and synthesized  $\text{CsPb}_2\text{Br}_5$  nanowires in water. We have proved that both  $\text{CsPb}_2\text{Br}_5$  and  $\text{CsPb}_2\text{Br}_{5-\gamma}\text{X}_\gamma$  nanowires are non emissive and can be used as

optical waveguides. We have also shown that the decorated  $\text{CsPbBr}_{3-\gamma}\text{X}_\gamma$  nanocrystals are responsible for the strong emission from  $\text{CsPb}_2\text{Br}_{5-\gamma}\text{X}_\gamma$  nanowires.  $\text{CsPbBr}_3$  and  $\text{CsPbBr}_{3-\gamma}\text{X}_\gamma$  nanocrystals can spontaneously grow on the surface of  $\text{CsPb}_2\text{Br}_{5-\gamma}\text{X}_\gamma$  nanowires. Although the location of  $\text{CsPbBr}_{3-\gamma}\text{X}_\gamma$  nanocrystals on nanowires remains random, a precise position of nanocrystals can be achieved. For example, we can deposit a nanoscale droplet of  $\text{CsPbBr}_{3-\gamma}\text{X}_\gamma$  aqueous solution on the nanowires using an AFM tip.<sup>[57,58]</sup> The intimate integration of lead halide nanocrystals to lead halide nanowire waveguides provides us new opportunities for wider device applications of highly luminescent perovskite nanocrystals.

### 4. Experimental Section

*The Synthesis of  $\text{CsPbBr}_3$  and  $\text{CsPbBr}_{3-\gamma}\text{X}_\gamma$  ( $\text{X} = \text{Cl}$  or  $\text{I}$ ) Powder:*  $\text{CsPbBr}_3$  microcubes (or powders) were synthesized using a modified method by mixing 4 mmol  $\text{Pb}(\text{CH}_3\text{COO})_2 \cdot 3\text{H}_2\text{O}$  and 8 mmol  $\text{CsBr}$  in 10 mL 48% HBr solution ( $\approx$  90 mmol) at room temperature and stirred for about 1 h.  $\text{CsPbBr}_{3-\gamma}\text{X}_\gamma$  ( $\text{X} = \text{Cl}$  or  $\text{I}$ ) powder was synthesized by mixing 4 mmol  $\text{Pb}(\text{CH}_3\text{COO})_2 \cdot 3\text{H}_2\text{O}$ , 2 mmol  $\text{CsCl}$  (or  $\text{CsI}$ ), and 6 mmol  $\text{CsBr}$  in a solution containing 90 mmol  $\text{HCl}$  (or  $\text{HI}$ ) and 270 mmol HBr.

*XRD:* XRD patterns of the samples were recorded on DX-2700BH X-ray diffractometer with a  $\text{Cu K}\alpha$  source.

*SEM/TEM:* SEM images were recorded on Nova Nano scanning electron microscope 450. TEM images were recorded on FEI Titan ETEM G2 80-300.

*Raman/PL:* Raman spectra and PL spectra were performed with Horiba LabSpec 6 which can measure Raman and PL on the same spot of a sample.

### Supporting Information

Supporting Information is available from the Wiley Online Library or from the author.

## Acknowledgements

T.C. and C.W. contributed equally to this work. C.W. would like to thank the financially support of the National Natural Science Foundation of China [No. 12164051 and No. 11564043], Joint Foundation of Provincial Science and Technology Department-Double First-class Construction of Yunnan University [No. 2019FY003016] and Young Top Talent Project of Yunnan Province [No. YNWR-QNB-2018-229]. T.C. thanks Advanced Analysis and Measurement Center of Yunnan University for the sample characterization service. J.M.B. acknowledges support from the Robert A. Welch Foundation (E-1728). The TEM work at Purdue was supported by the U.S. National Science Foundation (DMR-2016453 and DMR-1565822). Work at the Molecular Foundry (H. A. Calderon) was supported by the Office of Science, Office of Basic Energy Sciences, of the U.S. Department of Energy under Contract No. DE-AC02-05CH11231. J.Y. would like to thank the financially support of the National Natural Science Foundation of China [No. 62064013], the Application Basic Research Project of Yunnan Province [No. 2019FB130].

## Conflict of Interest

The authors declare no conflict of interest.

## Data Availability Statement

The data that support the findings of this study are available from the corresponding author upon reasonable request.

## Keywords

*CsPb<sub>2</sub>Br<sub>5</sub>* nanowires, dissolution–recrystallization, luminescence, morphological transformation, nanowire waveguide integration

Received: August 20, 2021

Revised: December 8, 2021

Published online: January 20, 2022

- [1] M. A. Becker, R. Vaxenburg, G. Nedelcu, P. C. Sercel, A. Shabaev, M. J. Mehl, J. G. Michopoulos, S. G. Lambrakos, N. Bernstein, J. L. Lyons, T. Stoferle, R. F. Mahrt, M. V. Kovalenko, D. J. Norris, G. Raino, A. L. Efros, *Nature* **2018**, *553*, 189.
- [2] Y. Cao, N. Wang, H. Tian, J. Guo, Y. Wei, H. Chen, Y. Miao, W. Zou, K. Pan, Y. He, H. Cao, Y. Ke, M. Xu, Y. Wang, M. Yang, K. Du, Z. Fu, D. Kong, D. Dai, Y. Jin, G. Li, H. Li, Q. Peng, J. Wang, W. Huang, *Nature* **2018**, *562*, 249.
- [3] Y. Zhang, J. Liu, Z. Wang, Y. Xue, Q. Ou, L. Polavarapu, J. Zheng, X. Qi, Q. Bao, *Chem. Commun.* **2016**, *52*, 13637.
- [4] A. V. Akimov, A. Mukherjee, C. L. Yu, D. E. Chang, A. S. Zibrov, P. R. Hemmer, H. Park, M. D. Lukin, *Nature* **2007**, *450*, 402.
- [5] D. E. Chang, A. S. Sørensen, P. R. Hemmer, M. D. Lukin, *Phys. Rev. B* **2007**, *76*, 035420.
- [6] A. Imamoglu, D. D. Awschalom, G. Burkard, D. P. DiVincenzo, D. Loss, M. Sherwin, A. Small, *Phys. Rev. Lett.* **1999**, *83*, 4204.
- [7] F. Gu, H. Yu, P. Wang, Z. Yang, L. Tong, *ACS Nano* **2010**, *4*, 5332.
- [8] K. Hennessy, A. Badolato, M. Winger, D. Gerace, M. Atature, S. Gulde, S. Falt, E. L. Hu, A. Imamoglu, *Nature* **2007**, *445*, 896.
- [9] P. J. Cegielski, S. Neutzner, C. Porschatis, H. Lerch, J. Bolten, S. Suckow, A. R. S. Kandada, B. Chmielak, A. Petrozza, T. Wahlbrink, A. L. Giesecke, *Opt. Express* **2017**, *25*, 13199.
- [10] J. Zhang, Y. H. Ye, X. Wang, P. Rochon, M. Xiao, *Phys. Rev. B* **2005**, *72*, 201306.
- [11] Z. Hirboodvash, M. Khodami, N. R. Fong, E. Lisicka-Skrzek, A. Olivieri, H. Northfield, R. N. Tait, P. Berini, *Appl. Opt.* **2019**, *58*, 2994.
- [12] D. Chatzitheocharis, D. Ketzaki, C. Calo, C. Caillaud, K. Vrysokinos, *Opt. Express* **2020**, *28*, 34219.
- [13] O. H. Cheng, T. Qiao, M. Sheldon, D. H. Son, *Nanoscale* **2020**, *12*, 13113.
- [14] K. Lin, J. Xing, L. N. Quan, F. P. G. de Arquer, X. Gong, J. Lu, L. Xie, W. Zhao, D. Zhang, C. Yan, W. Li, X. Liu, Y. Lu, J. Kirman, E. H. Sargent, Q. Xiong, Z. Wei, *Nature* **2018**, *562*, 245.
- [15] D. D. Zhang, S. W. Eaton, Y. Yu, L. T. Dou, P. D. Yang, *J. Am. Chem. Soc.* **2015**, *137*, 9230.
- [16] C. Fan, X. Xu, K. Yang, F. Jiang, S. Wang, Q. Zhang, *Adv. Mater.* **2018**, *30*, 1804707.
- [17] Y. Meng, Z. Lai, F. Li, W. Wang, S. Yip, Q. Quan, X. Bu, F. Wang, Y. Bao, T. Hosomi, T. Takahashi, K. Nagashima, T. Yanagida, J. Lu, J. C. Ho, *ACS Nano* **2020**, *14*, 12749.
- [18] Z. Gu, W. Sun, K. Wang, N. Zhang, C. Zhang, Q. Lyu, J. Li, S. Xiao, Q. Song, *J. Mater. Chem. A* **2016**, *4*, 8015.
- [19] S. Zou, G. Yang, T. Yang, D. Zhao, Z. Gan, W. Chen, H. Zhong, X. Wen, B. Jia, B. Zou, *J. Phys. Chem. Lett.* **2018**, *9*, 4878.
- [20] H. Utzat, W. Sun, A. E. K. Kaplan, F. Krieg, M. Ginterseder, B. Spokony, N. D. Klein, K. E. Shulenberger, C. F. Perkins, M. V. Kovalenko, M. G. Bawendi, *Science* **2019**, *363*, 1068.
- [21] R. Uppu, H. T. Eriksen, H. Thyrrestrup, A. D. Ugurlu, Y. Wang, S. Scholz, A. D. Wieck, A. Ludwig, M. C. Lobl, R. J. Warburton, P. Lodahl, L. Midolo, *Nat. Commun.* **2020**, *11*, 3782.
- [22] G. P. Li, H. Wang, Z. F. Zhu, Y. J. Chang, T. Zhang, Z. H. Song, Y. Jiang, *Chem. Commun.* **2016**, *52*, 11296.
- [23] J. Yin, G. Zhang, X. Tao, *CrystEngComm* **2019**, *21*, 1352.
- [24] Z. Zhang, Y. Zhu, W. Wang, W. Zheng, R. Lin, F. Huang, *J. Mater. Chem. C* **2018**, *6*, 446.
- [25] I. Dursun, M. De Bastiani, B. Turedi, B. Alamer, A. Shkurenko, J. Yin, A. M. El-Zohry, I. Gereige, A. AlSaggaf, O. F. Mohammed, M. Eddaoudi, O. M. Bakr, *ChemSusChem* **2017**, *10*, 3746.
- [26] P. Acharyya, P. Pal, P. K. Samanta, A. Sarkar, S. K. Pati, K. Biswas, *Nanoscale* **2019**, *11*, 4001.
- [27] C. Wang, Y. Wang, X. Su, V. G. Hadjiev, S. Dai, Z. Qin, H. A. Calderon Benavides, Y. Ni, Q. Li, J. Jian, M. K. Alam, H. Wang, F. C. R. Hernandez, Y. Yao, S. Chen, Q. Yu, G. Feng, Z. Wang, J. Bao, *Adv. Mater.* **2019**, *31*, 1902492.
- [28] H. Huang, H. Lin, S. V. Kershaw, A. S. Susha, W. C. H. Choy, A. L. Rogach, *J. Phys. Chem. Lett.* **2016**, *7*, 4398.
- [29] D. Zhang, Y. Yang, Y. Bekenstein, Y. Yu, N. A. Gibson, A. B. Wong, S. W. Eaton, N. Kornienko, Q. Kong, M. Lai, A. P. Alivisatos, S. R. Leone, P. Yang, *J. Am. Chem. Soc.* **2016**, *138*, 7236.
- [30] L. Ruan, W. Shen, A. Wang, Q. Zhou, H. Zhang, Z. Deng, *Nanoscale* **2017**, *9*, 7252.
- [31] J. Chen, J. Wang, X. Xu, J. Li, J. Song, S. Lan, S. Liu, B. Cai, B. Han, J. T. Precht, D. Ginger, H. Zeng, *Nat. Photonics* **2020**, *15*, 238.
- [32] X. Zhang, B. Xu, J. Zhang, Y. Gao, Y. Zheng, K. Wang, X. W. Sun, *Adv. Funct. Mater.* **2016**, *26*, 4595.
- [33] Z. Huang, B. Ma, H. Wang, N. Li, R. Liu, Z. Zhang, X. Zhang, J. Zhao, P. Zheng, Q. Wang, H. Zhang, *J. Phys. Chem. Lett.* **2020**, *11*, 6007.
- [34] B. S. Zhu, H. Z. Li, J. Ge, H. D. Li, Y. C. Yin, K. H. Wang, C. Chen, J. S. Yao, Q. Zhang, H. B. Yao, *Nanoscale* **2018**, *10*, 19262.
- [35] Z.-L. Yu, Y.-Q. Zhao, Q. Wan, B. Liu, J.-L. Yang, M.-Q. Cai, *J. Phys. Chem. C* **2020**, *124*, 23052.
- [36] S. Cho, S. H. Yun, *Commun. Chem.* **2020**, *3*, 15.
- [37] S. Lou, Z. Zhou, W. Gan, T. Xuan, Z. Bao, S. Si, L. Cao, H. Li, Z. Xia, J. Qiu, R.-S. Liu, J. Wang, *Green Chem.* **2020**, *22*, 5257.
- [38] M. Cao, Y. Damji, C. Zhang, L. Wu, Q. Zhong, P. Li, D. Yang, Y. Xu, Q. Zhang, *Small Methods* **2020**, *4*, 2000303.

[39] K. Wang, L. Wu, L. Li, H. Yao, H. Qian, S. Yu, *Angew. Chem., Int. Ed.* **2016**, *55*, 8328.

[40] L. Zhang, K. Wang, Y. Lin, B. Zou, *J. Phys. Chem. Lett.* **2020**, *11*, 4693.

[41] Y. Q. Zhou, J. Xu, J. B. Liu, B. X. Liu, *J. Phys. Chem. Lett.* **2019**, *10*, 6118.

[42] L. Ruan, J. Lin, S. Shen, Z. Deng, *Nanoscale* **2018**, *10*, 7658.

[43] L. Ruan, W. Shen, A. Wang, A. Xiang, *J. Phys. Chem. Lett.* **2017**, *8*, 3853.

[44] B. Turedi, K. J. Lee, I. Dursun, B. Alamer, Z. Wu, E. Alarousu, O. F. Mohammed, N. Cho, O. M. Bakr, *J. Phys. Chem. C* **2018**, *122*, 14128.

[45] H. Dong, S. Kareem, X. Gong, J. Ruan, P. Gao, X. Zhou, X. Liu, X. Zhao, Y. Xie, *ACS Appl. Mater. Interfaces* **2021**, *13*, 23960.

[46] R. Wang, Z. Li, S. Li, P. Wang, J. Xiu, G. Wei, H. Liu, N. Jiang, Y. Liu, M. Zhong, *J. Phys. Chem. C* **2018**, *122*, 14128.

[47] G. Maity, S. K. Pradhan, *J. Alloys Compd.* **2020**, *816*, 152612.

[48] L. Wu, H. Hu, Y. Xu, S. Jiang, M. Chen, Q. Zhong, D. Yang, Q. Liu, Y. Zhao, B. Sun, Q. Zhang, Y. Yin, *Nano Lett.* **2017**, *17*, 5799.

[49] L. Wang, G. Liu, L. Zou, D. Xue, *J. Alloys Compd.* **2010**, *493*, 471.

[50] Y. Sun, B. Mayers, T. Herricks, Y. Xia, *Nano Lett.* **2003**, *3*, 955.

[51] X. Xia, S. Xie, M. Liu, H. Peng, N. Lu, J. Wang, M. J. Kim, Y. Xia, *Proc. Natl. Acad. Sci. USA* **2013**, *110*, 6669.

[52] L. Yan, R. Yu, J. Chen, X. Xing, *Cryst. Growth Des.* **2008**, *8*, 1474.

[53] Y. Tong, B. J. Bohn, E. Bladt, K. Wang, P. Müller-Buschbaum, S. Bals, A. S. Urban, L. Polavarapu, J. Feldmann, *Angew. Chem., Int. Ed.* **2017**, *56*, 13887.

[54] I. Pastoriza-Santos, L. M. Liz-Marzán, *Langmuir* **2002**, *18*, 2888.

[55] Z. A. Peng, X. Peng, *J. Am. Chem. Soc.* **2002**, *124*, 3343.

[56] W. H. Lai, Y. X. Wang, Y. Wang, M. Wu, J. Z. Wang, H. K. Liu, S. L. Chou, J. Chen, S. X. Dou, *Nat. Chem.* **2019**, *11*, 695.

[57] P. Galliker, J. Schneider, H. Eghlidi, S. Kress, V. Sandoghdar, D. Poulikakos, *Nat. Commun.* **2012**, *3*, 890.

[58] K. Kaisei, N. Satoh, K. Kobayashi, K. Matsushige, H. Yamada, *Nanotechnology* **2011**, *22*, 175301.